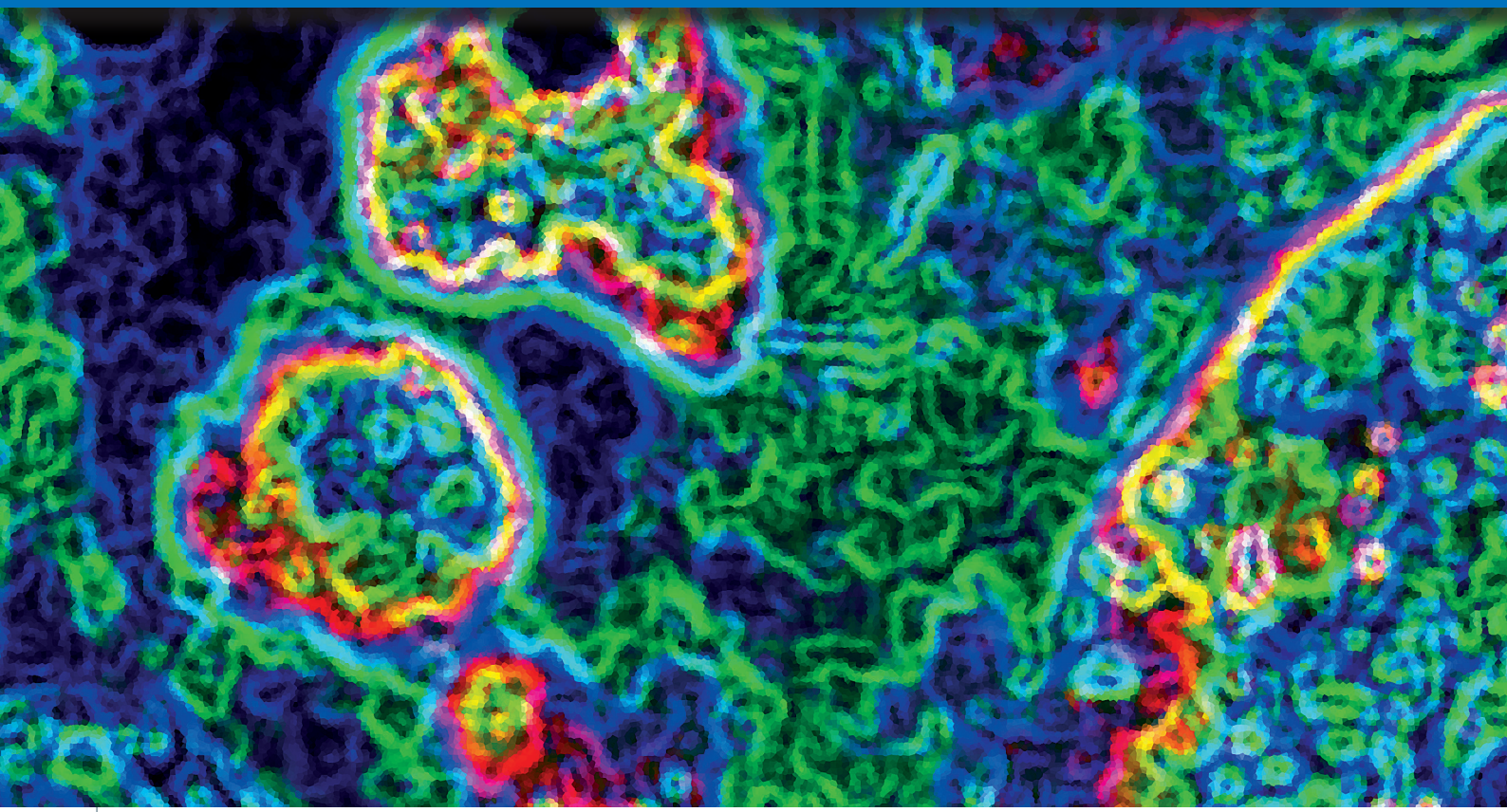

MALDI FTMS Imaging Mass Spectrometry of N-glycans as Tissue Biomarkers of Cancer

In this application note, we describe preparation and imaging analysis of N-glycans from formalin-fixed paraffin embedded (FFPE) tissues using the solariX MALDI FTMS.

N-glycosylation is a common post translational modification consisting of a carbohydrate moiety attached to the consensus sequence Asn-X-Ser/Thr, where X may be any amino acid residue other than proline, and a frequent modification of membrane associated proteins. N-glycans are synthesized and processed in the ER and Golgi through the activity of over 300 enzymes that attach or trim sugar residues, resulting in thousands of different structural combinations (1). The large structural diversity of N-glycans plays a role in fine tuning protein structure and function. Cellular activities that depend on N-glycosylation include protein folding, protein targeting, regulation of protease activity, cell migration and cell-cell recognition (2, 3).

Keywords: glycans, MALDI, Imaging, FTMS, solarix

Authors: Peggi M. Angel, Anand S. Mehta, Richard R. Drake.
Dept. of Cell and Molecular Pharmacology & Experimental Therapeutics, Medical University of South Carolina, Charleston, SC

In cancer, N-glycosylation plays a critical role in the tumor microenvironment, mediating inflammatory and immune response, altering extracellular matrix production, and modulating cell surface receptor and stroma-tumor interactions. N-glycosylation alterations thus serve as important biomarkers and targets of therapy regulating the development and progression of cancer (4).

Recently, methods for using MALDI imaging mass spectrometry to evaluate the N-glycome from FFPE thin tissue sections were reported (5, 6). The developed workflow is amenable for evaluation of the vast numbers of stored FFPE clinical samples towards new studies in cancer diagnosis and prognosis (7). Although N-glycan imaging may be accomplished with any MALDI imaging mass spectrometry platform, there are certain advantages

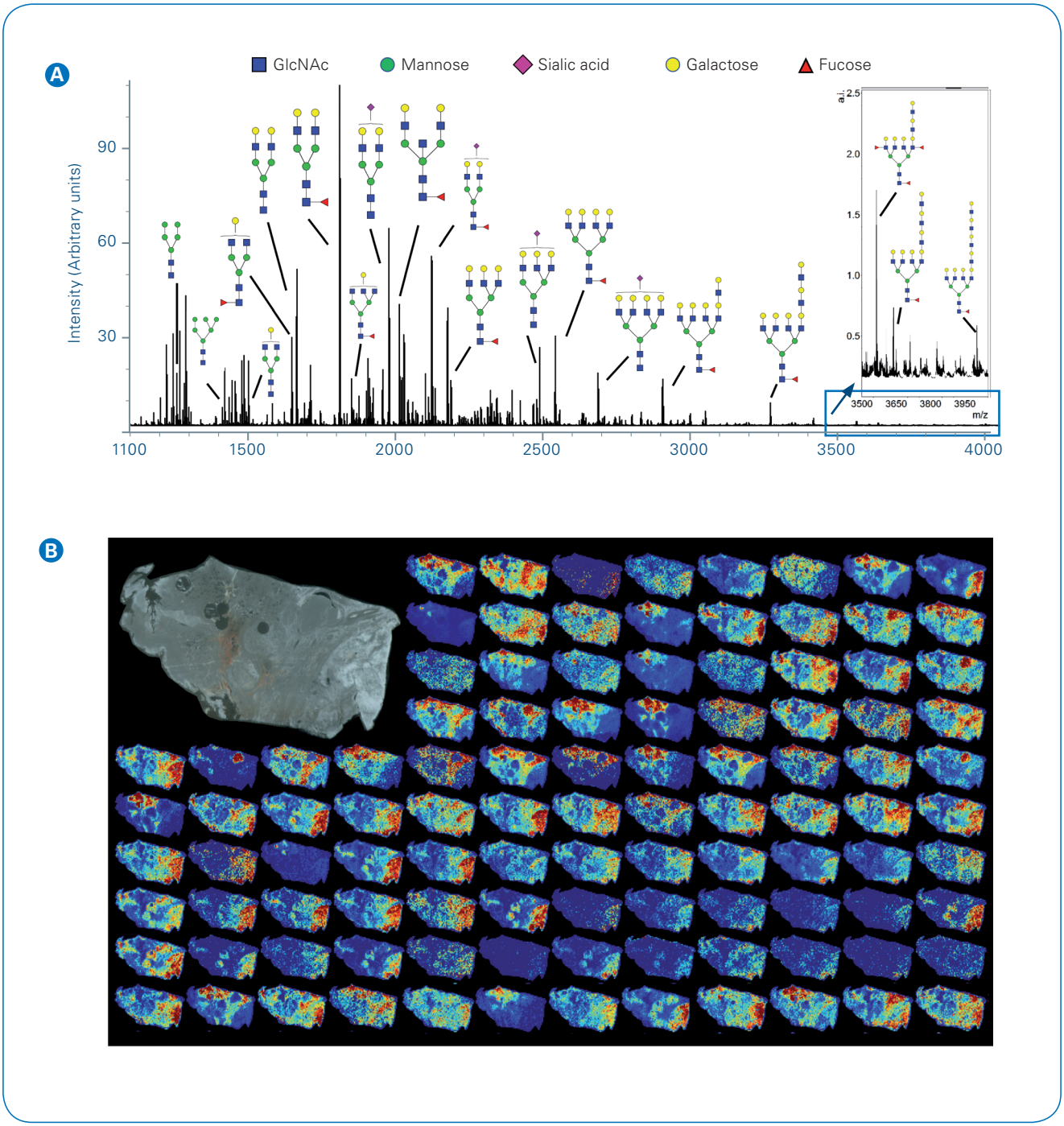

Figure 1. Example N-glycan signal from a single section of thyroid cancer. A Total average spectrum from the image with example glycoform structures per m/z; B Tile view of example images. Inset top right, photomicrograph of unstained tissue prior to imaging. Abbreviations: GlcNAc, N-acetylglucosamine

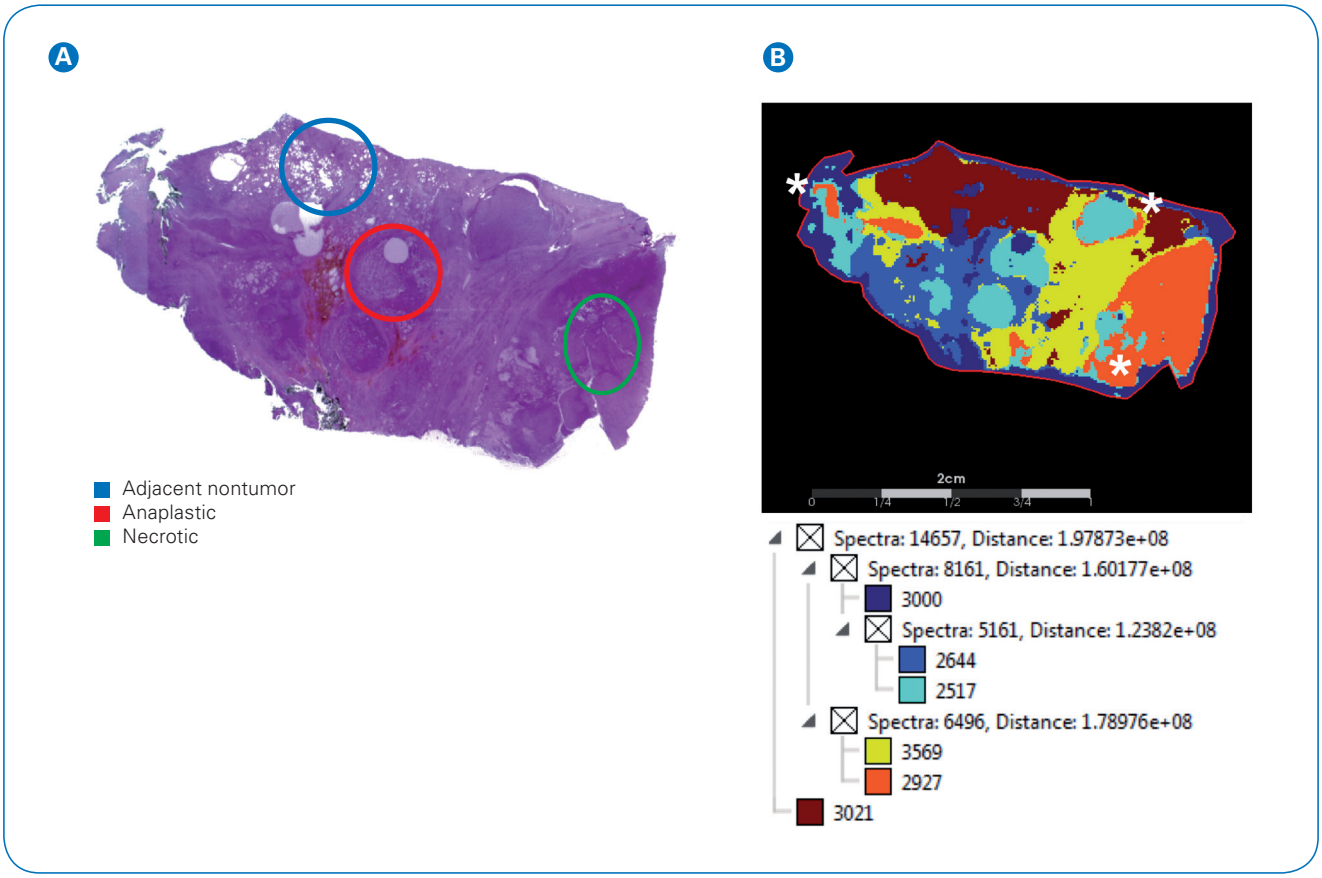

Figure 2. Image segmentation showing complexity of N-glycan signatures in a thyroid cancer tissue section. A Pathologist marked H&E stain of section highlighting adjacent nontumor, anaplastic, and necrotic regions. B SCiLS image segmentation of N-glycans from 2D mapping. White asterisks mark calculated overlaps of anaplastic and necrotic regions.

to using the solariX MALDI FTMS. In this note, we discuss high sensitivity mapping of the N-glycome as detected from the complex tissue environment of an FFPE thyroid cancer specimen.

Methods

Methods for releasing N-glycans from FFPE tissue have been described in detail (5). Use of de-identified tissue specimens to be discarded was approved by an Institutional Review Board. Briefly, a 5 µm thick FFPE tissue section of thyroid cancer was incubated for one hour at 60°C, dewaxed, and antigen retrieved under acidic conditions (10 mM citraconic buffer, pH 3). A robotic sprayer (TM-Sprayer™, HTXImaging) was used to apply the enzyme and matrix in separate steps. First, recombinant PNGase F (Mehta Lab, Medical University of South Carolina) was sprayed onto tissue at 0.1 µg/µL. The sample was then incubated in a closed cell culture dish at 37°C under high humidity for two hours. Afterwards, α-cyano-4-hydroxycinnamic acid (CHCA) was sprayed onto tissue at 7 mg/mL in 50% acetonitrile, 0.1% trifluoroacetic acid.

MALDI imaging analysis was performed in positive ion mode using a 7 T solariX equipped with a dual ESI/MALDI ion source and a Smartbeam II laser set to minimum focus. A total of 200 laser shots were collected at each pixel with a spacing of 150 µm between each pixel. Images were collected in broadband mode spanning m/z 500-5,000, with a transient length of 1.2 seconds, resulting in an on-tissue resolving power of approximately 85,000 at m/z 1,850. FlexImaging software version 4.1 was used to produce a peak list linked to 2D tissue maps. N-glycans were putatively identified based on accurate mass within 5 ppm using GlycoWorkbench 2.0.(8) The 2D data and peak lists were uploaded to SCiLS Lab software (2016b, Version 4.01.8705, Bruker Daltonics) for analysis between pathologist marked tumor and nontumor regions. For image segmentation, SCiLS parameters used were weak denoising, bisecting K-means, and the Manhattan metric. Altered N-glycans were filtered by Wilcoxon rank sum hypothesis testing p value ≤1.0E-3 and area under the receiver operating curve ≤0.8.

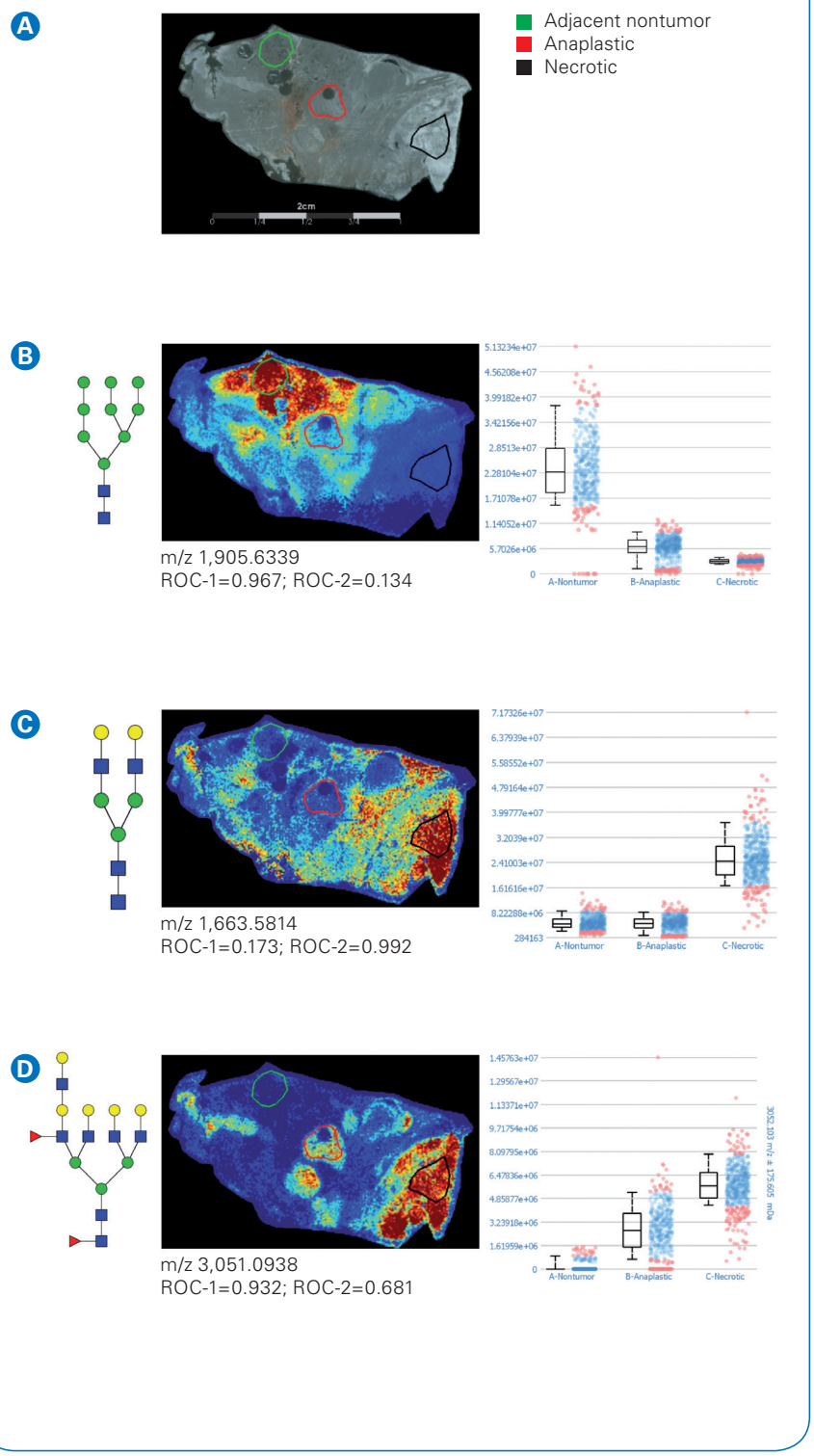

Figure 3. Quantification of N-glycan signatures from regional areas on tissue. Statistical testing was done comparing nontumor adjacent and anaplastic regions (ROC-1) or anaplastic versus necrotic (ROC-2). **A** *Photomicrograph depicting areas selected for measuring relative abundance of N-glycan expression.* **B** *A high mannose (Man9) structure distinguishing nontumor adjacent compared to anaplastic tumor or necrotic regions.* **C** *A biantennary N-glycan defining necrotic regions with low expression in nontumor adjacent and anaplastic.* **D** *A tetrantennary fucosylated structure with low expression in adjacent nontumor and increasing expression in anaplastic and necrotic tissues regions.*

Results and Discussion

In this work, we demonstrate N-glycan imaging analysis using a tissue section containing anaplastic thyroid cancer. Thyroid cancer is the most common malignancy of the endocrine system. Most thyroid cancers remain stable and indolent and patients have a good outcome when treated by surgical resection or therapies directed at inhibiting growth promoting kinases and angiogenesis (9). Anaplastic thyroid tumors are the least common but the most deadly form of thyroid cancer, and most patients die within a year. Prognosis is poor due to a lack of effective therapies and new molecular information is sought to develop therapies that stop tumor progression.

The example tissue section of an anaplastic thyroid cancer was prepared using our standard protocol for N-glycan release and analyzed by MALDI FTMS using a 7.0 Tesla solariX. Figure 1 shows total ion current and examples of 2D N-glycans mapped across the tissue. Detection of N-glycans is entirely dependent on the activity of the applied PNGase F. Here, over 111 N-glycans were detected as $[M+Na]^+$ or $[M-H+2Na]^+$, including high mannose, complex, hybrid, and sialylated structures. It is important to note that sialic acids are thermally labile and most MALDI sources result in loss of the sialic acid from the N-glycan. The solariX was designed specifically to minimize loss of sialic acids using high pressure collisional cooling gas (10). As a result, sialylated N-glycans are detected with equivalent intensity to N-glycans that do not contain this labile residue (Figure 1A). A second advantage using the solariX is that the source is decoupled from the mass measurement so that tissues mounted on standard microscope slides may be analyzed with negligible loss of mass resolution or mass

accuracy. Here, the combined workflow and imaging platform yield high sensitivity detection of a broad m/z range of N-glycans, spanning from small pentamannose structures (Man5, m/z 1,257.4226) to fucosylated tetraantennary species with extended poly-N-acetyllactosamine (polyLacNAc) series (m/z 4,000.4325). Overall, the N-glycan imaging workflow produces intense and comprehensive N-glycan signatures from FFPE tissue. In general, we have observed that the analysis of advanced tumors (like this example) have N-glycan signatures that allow mapping of well over 100 N-glycan species.

SCiLS image segmentation was used to evaluate the imaged tissue in comparison to the pathologist marked tissue. Figure 2 shows the pathologist marked hematoxylin and eosin stain of the thyroid tissue, with regions marked as adjacent nontumor, necrotic or anaplastic tumor. Segments were manually expanded to give equivalent numbers of spectra per region. Comparison of pathologist marked sections to SCiLS segmentation highlights the complexity of the tumor environment. Specifically, segments match to pathologist markings of normal adjacent (dark red) and necrotic (orange), but show increased expansion of anaplastic tumor regions (aqua). However, N-glycan signatures mapping to the anaplastic region extend into the necrotic regions with some dispersion near adjacent non-tumor tissue. These data highlight that N-glycan signatures link to distinct tissue pathologies.

Tissue regions were selected from the pathologist marked regions to evaluate quantitative measurement of N-glycans (Figure 3). Regions were selected from within the pathologist marked areas for adjacent nontumor, necrotic, and anaplastic tumor. An example is shown of a high mannose structure (Man9) mapped to nonadjacent tissue areas with a ~ fourfold increase based on median value compared to anaplastic tumor regions. Necrotic regions showed unique signatures apart from both nonadjacent tumor and anaplastic tumor, shown here with an example biantennary structure. Interestingly, N-glycans found in anaplastic tumor regions were frequently also found in pathologist marked necrotic regions (see also Figure 1 B). These examples illustrate that N-glycan expression is uniquely regulated within the tumor micro-environment, and these alterations may be detected by the solariX MALDI FTMS imaging platform.

Conclusions

The N-glycan imaging workflow reveals complex carbohydrate interactions taking place within FFPE tumor tissues. An important component of the imaging workflow as illustrated here is the use of the solariX. The cooled source enables capturing biologically important but labile carbohydrate moieties, sialic acids, that would otherwise be lost in MALDI analysis. High sensitivity allows detection over a wide range of N-glycan structures. Analysis of this single piece of tissue section highlights the many unique N-glycosylation changes that can occur in anaplastic thyroid cancer. This workflow provides a valuable tool that allows deeper investigations into the molecular causes of disease, and can be applied to any FFPE tissue.

Learn More

You are looking for further Information? Check out the link or scan the QR code for our latest webinar.

www.bruker.com/drake-maldi-imaging

References

1. Moremen KW, Tiemeyer M, Nairn AV. 2012. Nature Reviews Molecular Cell Biology 13: 448-62
2. Stanley P, Schachter H, Taniguchi N. 2009. Chapter 8: N-Glycans. In Essentials of Glycobiology, ed. A Varki, RD Cummings, JD Esko, HH Freeze, P Stanley, et al. Cold Spring Harbor (NY): Cold Spring Harbor Laboratory Press
3. Varki A. 2017. Glycobiology 27: 3-49
4. Pinho SS, Reis CA. 2015. Nature Reviews Cancer 15: 540-55
5. Powers TW, Neely BA, Shao Y, Tang H, Troyer DA, et al. 2014. PLoS One 9: e106255, pp1-11. PMID: 25184632
6. Drake RR, Powers TW, Jones EE, Bruner E, Mehta AS, Angel PM. 2017. Advances in Cancer Research 134: 85-116
7. Gorzolka K, Walch A. 2014. Histology and Histopathology 29: 1365-76
8. Ceroni A, Maass K, Geyer H, Geyer R, Dell A, Haslam SM. 2008. Journal of Proteome Research 7: 1650-9
9. Lin R-Y. 2011. Nature Reviews Endocrinology 7: 609-16
10. O'Connor PB, Mirgorodskaya E, Costello CE. 2002. Journal of the American Society for Mass Spectrometry 13: 402-7

For Research Use Only. Not for Use in Clinical Diagnostic Procedures.

Bruker Daltonics GmbH & Co. KG

Bremen · Germany
Phone +49 (0)421-2205-0

Bruker Scientific LLC

Billerica, MA · USA
Phone +1 (978) 663-3660

ms.sales.bdal@bruker.com – www.bruker.com